# Ab initio studies of ClO x reactions. IV. Kinetics and mechanism for the self-reaction of ClO radicals

R. S. Zhu and M. C. Lin

---

**Articles you may be interested in**

Ab initio studies of ClO x reactions. IX. Combination and disproportionation reactions of ClO and s- ClO 3 radicals
J. Chem. Phys. 119, 8897 (2003); 10.1063/1.1613632

Ab initio studies of ClO x reactions. VIII. Isomerization and decomposition of ClO 2 radicals and related bimolecular processes
J. Chem. Phys. 119, 2075 (2003); 10.1063/1.1585027

Ab initio studies of ClO x reactions. I. Kinetics and mechanism for the OH + ClO reaction
J. Chem. Phys. 116, 7452 (2002); 10.1063/1.1467057

Ab initio study of the CH 3 + O 2 reaction: Kinetics, mechanism and product branching probabilities
J. Chem. Phys. 115, 195 (2001); 10.1063/1.1376128

Temperature and pressure dependence of the addition reactions of HO to NO and to NO 2 . IV. Saturated laser-induced fluorescence measurements up to 1400 bar
J. Chem. Phys. 108, 5391 (1998); 10.1063/1.475971

---

# *Ab initio* studies of ClO$_x$ reactions. IV. Kinetics and mechanism for the self-reaction of ClO radicals

R. S. Zhu and M. C. Lin[a)]
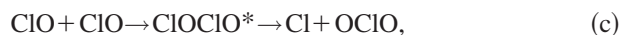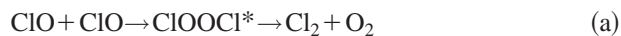*Department of Chemistry, Emory University, Atlanta, Georgia 30322*

The self-reaction of ClO radicals has been investigated by *ab initio* molecular orbital and variational transition state theory calculations. Both singlet and triplet potential energy surfaces were predicted by the modified Gaussian-2 method. The reaction was shown to take place mainly over the singlet surface by forming ClOOCl ($k_1$) and ClOClO ($k_{1'}$). These association processes were found to be strongly pressure dependent and the predicted total rate constants are in good agreement with the experimental data. The predicted second- and third-order rate constants for formation of ClOOCl and ClOClO can be expressed, respectively, in units of cm$^3$ molecule$^{-1}$ s$^{-1}$ and cm$^6$ molecule$^{-2}$ s$^{-1}$ by $k_1^\infty = 1.6 \times 10^{-9} T^{-0.67} \exp(-64/T)$, $k_{1'}^\infty = 6.4 \times 10^{-9} T^{-0.78} \exp(-76/T)$, and $k_1^0 = 8.31 \times 10^{-20} T^{-4.96} \exp(-336/T)$, $k_{1'}^0 = 1.72 \times 10^{-14} T^{-6.99} \exp(-926/T)$ in the temperature range 180–500 K for N$_2$ as the third body. The observed *T, P*-dependent data could be best accounted for with the heat of formation of ClOOCl, $\Delta_f H_0^o(\text{ClOOCl}) = 29.4 \pm 1$ kcal/mol. The formation of Cl$_2$+O$_2$ (2), Cl +ClOO (3), and Cl+OClO (4) products have been confirmed, with the predicted pressure-independent rate constants: $k_2 = 1.09 \times 10^{-13} T^{0.66} \exp(-1892/T)$; $k_3 = 1.36 \times 10^{-13} T^{0.77} \exp(-2168/T)$; $k_4 = 6.26 \times 10^{-11} T^{0.005} \exp(-2896/T)$, respectively, in units of cm$^3$ molecule$^{-1}$ s$^{-1}$, covering the temperature range 200–1500 K. These results are also in reasonable agreement with existing experimental kinetic data. © *2003 American Institute of Physics.*
[DOI: 10.1063/1.1540623]

## I. INTRODUCTION

The recombination and disproportionation reactions of ClO radicals have been investigated extensively on account of their relevance to the O$_3$-destruction chemistry in the stratosphere.[1–15] In principle, the reactions may take place via at least two long-lived intermediates; *viz.*

$$\text{ClO} + \text{ClO} \rightarrow \text{ClOOCl}^* \rightarrow \text{Cl}_2 + \text{O}_2 \tag{a}$$

$$\rightarrow \text{Cl} + \text{ClOO} \tag{b}$$

$$\text{ClO} + \text{ClO} \rightarrow \text{ClOClO}^* \rightarrow \text{Cl} + \text{OClO}, \tag{c}$$

where * denotes internal excitation. Potentially, a third intermediate, ClClO$_2$, may be formed in the reverse Cl+OClO reaction, analogous to the association of OH with OClO, in which chloric acid (HOClO$_2$) may be a major product, depending on the pressure of the system.[16]

Under higher pressure conditions, particularly at low temperatures, collisional deactivation of excited association products producing ClOOCl and ClOClO may be important kinetically. In fact, for the most stable intermediate, ClOOCl, its formation is the dominant process under the stratospheric condition.[4,5,9,11,13,15] On the other hand, the disproportionation processes producing ClOO and OClO by (b) and (c), respectively, are endothermic by 3–4 kcal/mol (*vide infra*); accordingly, they cannot compete effectively with the recombination reaction in the stratosphere (with low temperature

and medium pressure). These endothermic reactions may, however, become dominant processes in the combustion of ammonium perchlorate (AP) propellant.

The effects of temperature and pressure on the total rate constant and product branching probabilities over a wide range of practical *T, P*-conditions (200 K$<T<$3000 K, 0 $<P<$200 atm) cannot be realistically studied in any laboratory experiments. In this series of theoretical studies,[17–19] we have employed high-level *ab initio* molecular orbital methods in conjunction with statistical theory calculations to map out the detailed potential energy surfaces (PES) involved and calculate the associated rate constants and product branching ratios for applications over a wide range of conditions relevant to specific practical requirements. For the three distinctly different systems, OH+ClO$_3$,[17] OH+ClO,[18] and O +OClO,[19] which we have investigated recently, the results have been very encouraging. We could not only quantitatively account for the experimentally determined total rate constants for these reactions, but also reliably predict the reported product branching ratios, typically measured under experimentally more readily accessible conditions.

Comparison between theory and experiment for a certain experimental condition does provide a much needed calibration of the computed energies and the overall mechanism involved for a more reliable extrapolation to more extreme practical conditions (e.g., at 1000–2500 K and 1–200 atm for AP combustion). In the present study, we have examined the effects of temperature and pressure on the recombination and disproportionation of ClO radicals combining *ab initio* MO and VRRKM calculations with a special emphasis on

---

[a)]National Science Council Distinguished Visiting Professor at Chiaotung University, Hsinchu, Taiwan. Electronic mail: chemmcl@emory.edu

the variation of product formation channels with temperature, from 200 K of interest to stratosphere to 3000 K of importance to AP combustion.

## II. COMPUTATIONAL METHODS

The geometry of the reactants, products, intermediates, and transition states of the title reaction have been fully optimized by using the hybrid density functional B3LYP method (Becke's three-parameter nonlocal exchange functional[20,21] with the correlation functional of Lee, Yang, and Parr[22]) with the $6\text{-}311+\text{G}(3df)$ basis set. Vibrational frequencies employed to characterize stationary points, zero-point energy (ZPE) corrections have also been calculated at this level of theory, and have been used for the rate constant calculations. All the stationary points have been positively identified for local minima (with the number of imaginary frequencies NIMAG$=0$) and transition states (with NIMAG$=1$). Intrinsic reaction coordinate (IRC) calculations[23] have been performed to confirm the connection of each transition state with designated intermediate.

The total G2M energy with zero-point energy (ZPE) correction is calculated as follows:[24]

$$E[(\text{G2M(CC2)})] = E_{\text{bas}} + \Delta E(+) + \Delta E(2df)$$
$$+ \Delta E(\text{CC}) + \Delta' + \Delta E(\text{HLC,CC2})$$
$$+ \text{ZPE}(3df),$$

$$E_{\text{bas}} = E[\text{PMP4/6-311G}(d,p)],$$

$$\Delta E(+) = E[\text{PMP4/6-311}+\text{G}(d,p)] - E_{\text{bas}},$$

$$\Delta E(2df) = E[\text{PMP4/6-311G}(2df,p)] - E_{\text{bas}},$$

$$\Delta E(\text{CC}) = E[\text{CCSD(T)/6-311G}(d,p)] - E_{\text{bas}},$$

$$\Delta' = E[\text{UMP2/6-311}+\text{G}(3df,2p)]$$
$$- E[\text{UMP2/6-311G}(2df,p)]$$
$$- E[\text{UMP2/6-311}+\text{G}(d,p)]$$
$$+ E[\text{UMP2/6-311G}(d,p)],$$

$$\Delta E(\text{HLC,CC2}) = -5.78n_\beta - 0.19n_\alpha$$

in units of mhartree,

where $n_\alpha$ and $n_\beta$ are the numbers of valence electrons, $n_\alpha \geq n_\beta$. All calculations were carried out with GAUSSIAN 98.[25]

The rate constants were computed with a microcanonical variational RRKM (VARIFLEX[26]) code, which solves the master equation[27,28] involving multistep vibrational energy transfers for the excited intermediate ClOOCl$^\dagger$ or ClOClO$^\dagger$. The energies for the intermediates and transition states calculated at the G2M (CC2) level were used in the calculation.

For the barrierless transition states, the Morse potential

$$E(R) = D_e[1 - e^{-\beta(R-Re)}]^2,$$

was used to represent the potential energy along the minimum energy path of each individual reaction coordinate. In the above equation, $R$ is the reaction coordinate (i.e., the distance between the two bonding atoms, O–O or O–Cl in this work), $D_e$ is the bond energy excluding zero-point en-

ergy, and $R_e$ is the equilibrium value of $R$. For the tight transition states, the numbers of states were evaluated according to the rigid-rotor harmonic-oscillator approximation.

For the formation of higher barrier disproportionate products in reactions (a) to (c), we have employed the CHEM-RATE code of Mokrushin et al.[29] to couple all low-lying reaction channels including isomerization processes by solving the $T, P$-dependent master equation.

## III. RESULTS AND DISCUSSION

### A. Potential energy surface and reaction mechanism

The optimized geometries of the intermediates and transition states are shown in Figs. 1 and 2, respectively. The singlet and triplet potential energy diagrams obtained at the G2M//B3LYP/6-311+G$(3df)$ level are presented in Figs. 3 and 4. The predicted vibrational frequencies and rotational constants are summarized in Table I to compare with the available experimental vibrational frequencies of ClOOCl and its isomers.

#### 1. Cl$_2$O$_2$ isomers

*a. Equilibrium geometries and frequencies.* Theoretically, most investigators[30–38] focused their studies on the three low-lying isomers, ClOOCl, ClOClO, and ClClO$_2$. Lee et al.[37] have investigated these isomers using different methods and basis sets [including CCSD(T) with large ANO basis sets for single-point energies calculation]; they indicated that $f$-type basis functions are necessary to obtain accurate equilibrium geometries and frequencies. Christen et al.[38] showed that density functional theory (DFT) calculations using hybrid functionals with large basis sets reproduced the experimental data well.

In this section, the structures and frequencies of five isomers, ClOOCl, ClClO$_2$, ClOClO, OClClO, and OOClCl, labeled as LM1–LM5 in Fig. 1, calculated at the B3LYP/6-311+G$(3df)$, are compared with previously predicted values and available experimental data. The first isomer, ClOOCl, has $C_2$ symmetry; the predicted Cl–O bond length at the B3LYP/6-311+G$(3df)$ level, 1.748 Å, can be compared with the calculated values, 1.731,[37] 1.753,[37] 1.711,[37] 1.706,[38] 1.731,[38] 1.746 Å (Ref. 38) obtained at the MP2/TZ2P, CCSD(T)/TZ2P, MP2/TZ2Pf, MP2/cc-PVQZ, B3PW91/6-311+G$(3d2f)$, B3LYP/aug-cc-PVTZ$+d$ levels, respectively. Apparently, the Cl–O bond lengths predicted by DFT and CCSD(T) methods appear to be too long even with larger basis sets, but the value predicted by the MP2 method with big basis sets seems to be closer to the experimental value, 1.704 Å.[39] The O–O bond length obtained at the B3LYP/6-311+G$(3df)$ level, 1.361 Å, is 0.065 Å shorter than the experimental value[39] and can be compared with 1.421, 1.411, 1.407, 1.409, 1.354, and 1.371 Å using the above six methods, respectively. These data show that the predicted Cl–O and O–O bond lengths depend strongly on the size of the basis set and the method. All of the calculated ClOO bond angles and ClOOCl dihedral angles deviate from experimental values, 110.1° and 81.0°,[39] by approximately ±1–2° and ±1–3°, respectively. Calculations in Ref. 38 indicated that the HF method totally fails in
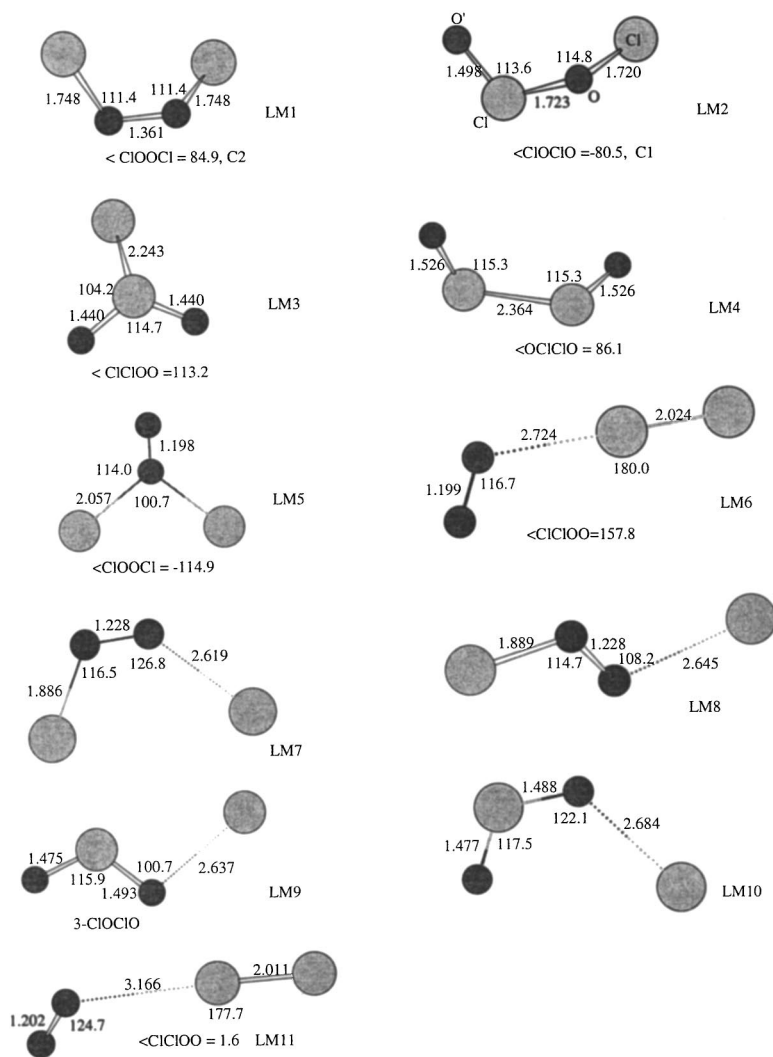
FIG. 1. The optimized geometry of intermediates computed at the B3LYP/6-311+G($3df$) level for the ClO+ClO reaction.

predicting the structure of ClOOCl. For the ClClO$_2$ isomer with $C_s$ symmetry, the Cl–Cl and Cl–O bond lengths, 2.243 and 1.440 Å obtained at the B3LYP/6-311+G($3df$) level are in good agreement with experimental values, 2.198 (Ref. 40) and 2.22,[41] and 1.436 (Ref. 40) and 1.440 Å,[41] respectively.

Our predicted Cl–Cl and Cl–O bond lengths are close to those values, 2.279, 1.468 Å; 1.202, 1.434 Å; 2.199, 1.429 Å obtained at the CCSD(T)/TZ2P,[37] B3PW91/6-311+G($3d2f$),[38] and B3PW91/cc-pVQZ[38] levels. For this structure, basis set and electron correlation effects are more important than that of ClOOCl.[37] For the ClOClO isomer, no experimental structure parameters are available. Calculations by either the DFT or the coupled-cluster method show that basis set has a strong effect on the middle ClO bond length. For instance, at the B3LYP/6-311G($d$) level it is 1.837 Å; with larger basis sets, it decreases to 1.737 Å (Ref. 38) and 1.723 Å (this work) at the B3LYP/cc-pVQZ and B3LYP/6-311($3df$) level, respectively. From CCSD(T)/DZP to CCSD(T)/TZ2P, the decrease is even larger, 0.126 Å.[37] This bond is also more sensitive to the correlation effect; for example, at the CCSD/TZ2P and CCSD(T)/TZ2P levels, the predicted values are 1.739 and 1.814 Å.[37] Again, this structure appears to be method dependent. The other two

isomers, OClClO and OOClCl, were previously optimized by Jensen and Oddershede[42] at the HF/3-21G* level, with no structure parameters available in their paper. Figure 1 shows the structural parameters of these two molecules with $C_2$ and $C_s$ symmetry at the B3LYP/6-311+G($3df$) level.

The frequencies of ClOOCl, ClClO$_2$, and ClOClO are shown in Table I. Our results at the B3LYP/6-311+G($3df$) level are similar to those obtained at the B3PW91/6-311+G($3d2f$)[38] and B3LYP/aug-cc-pVTZ+$d$.[38] From Table I one can see that the frequencies calculated at the B3LYP/6-311+G($3df$) level agree well with the experimental values of Müller et al.,[41] Chen and Lee,[43] and Jacobs and co-workers.[44] Many other complexes with loose structures, LM6–LM11, have also been located; they will be discussed in the following related parts.

*b. Relative energies.* Here, we mainly compare the stability of LM1 to LM5. The calculated G2M energies relative to ClO+ClO are presented in Fig. 3. The results show that the relative stability of the Cl$_2$O$_2$ isomers is approximately: ClOOCl≈ClClO$_2$>ClOClO>OClClO>OOClCl. At the G2M//B3LYP/6-311+G($3df$) level, ClOOCl lies 18.9 kcal/mol below the reactants, the dissociation energy ($D_0$) is the same as that predicted by Stanton et al.[33] using many-body perturbation theory (MBPT) and the infinite-order
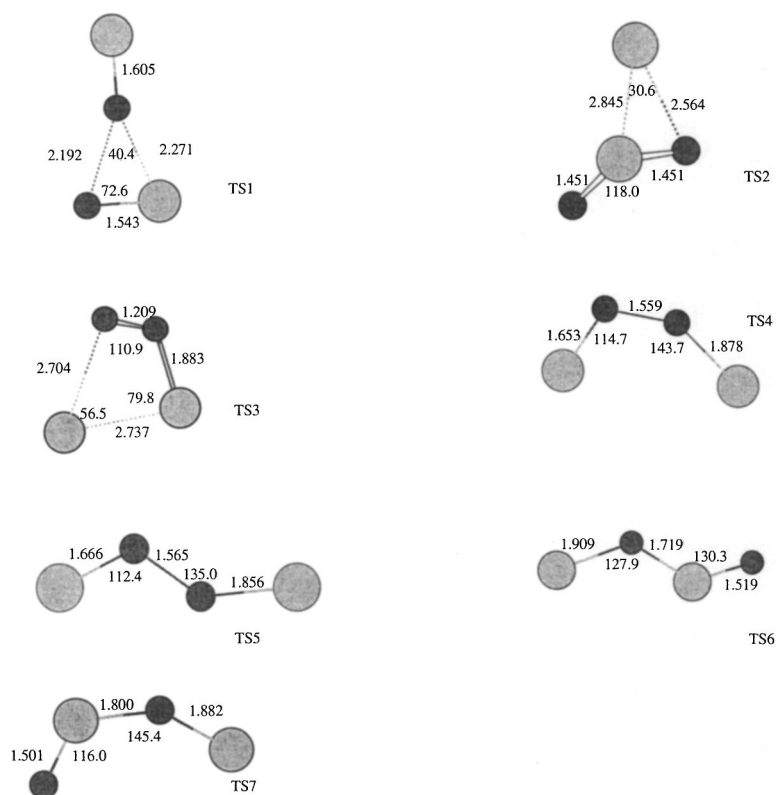
FIG. 2. The geometry of the transition states involved in the ClO+ClO reaction at the B3LYP/6-311 +G($3df$) level.

coupled-cluster (CC) approximation. The predicted value of $D_0$ (18.9 kcal/mol) is also close to the experimentally estimated enthalpy changes, 17.3,[9] 19.5,[13] and 18.1 (Ref. 13) kcal/mol at 200–300 K, corresponding to the values of 16.5, 18.6, and 17.2 reported at 0 K, but is different from the results computed at the G2 and CCSD(T)/[65321/54321]// CCSD/TZ2P levels, 22.1 kcal/mol[45] and 14.2 kcal/mol,[37] respectively. Further discussion on this important quantity will continue in the following section. For ClClO$_2$, which lies above ClOOCl by only 0.4 kcal/mol, the result is close to those relative to ClOOCl obtained by McGrath et al.[31] and Lee et al.,[37] 1.0 kcal/mol and 0.9±2.0 kcal/mol, respectively, but, according to Stanton et al.[33] and Li et al.,[45] ClOOCl is more stable than ClClO$_2$ by 6.7 and 7.7 kcal/mol, respectively. The third isomer, ClOClO, is predicted to be 7.0 kcal/mol less stable than ClOOCl; this energy difference is

the same as that reported by McGrath et al.[31] and also close to the best estimated result of Lee et al.,[37] 10.1 ±4 kcal/mol. At the G2 level, the energy difference was predicted to be 11.7 kcal/mol.[45] Finally, the other two isomers, OClClO and OOClCl, were predicted to lie 6.1 and 8.1 kcal/mol, respectively, above the reactants, as shown in Fig. 3. From the above comparison one can see that although uncertainties exist among the values computed by different methods, the relative stability of these isomers remains the same, i.e., ClOOCl≈ClClO$_2$>ClOClO≈OClClO ≈OOClCl.

  c. Isomerization. As OClClO and OOClCl have higher energies, only the isomerization processes involving the three low-lying isomers are investigated. TS1 and TS2 (see Figs. 2 and 3) correspond to the isomerization from ClOClO to ClOOCl and ClClO$_2$; they lie above the reactants by 0.5
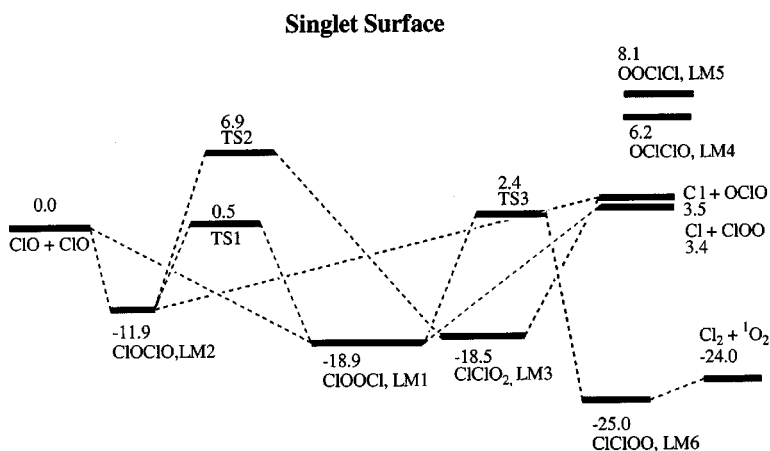


FIG. 3. The schematic diagram of the singlet potential energy surface for the ClO–ClO system computed at the G2M level.
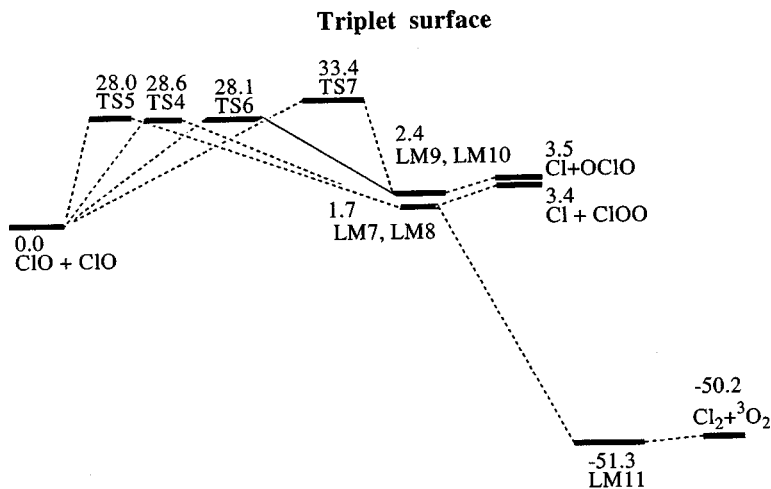
**Triplet surface**



FIG. 4. The schematic diagram of the triplet potential energy surface for the ClO–ClO system computed at the G2M level.

and 6.9 kcal/mol, respectively. The potential effect of the former isomerization process, which has a much smaller barrier, will be discussed later.

### 2. Formation of $ClO+ClO \rightarrow Cl_2 + {}^{1,3}O_2$

As discussed in the above section, many authors have theoretically investigated the structures and stabilities of the $Cl_2O_2$ isomers; however, the dissociation mechanisms of these isomers have not been reported before. In principle, $Cl_2 + {}^1O_2$ and ${}^3O_2$ can be produced via the singlet and triplet potential energy surfaces, respectively. Over the singlet surface, shown in Fig. 3, the ClOOCl intermediate can dissociate to give $Cl_2 + {}^1O_2$ via a four-center transition state TS3 in which the O–O bond length, 1.209 Å, is much close to that of ${}^1O_2$, 1.203 Å, obtained at the same level of theory. The breaking two Cl–O bonds lengthen unequally by 0.135 and 0.956 Å, compared with those in ClOOCl. TS3 lies 3.6 kcal/mol above the reactants; this value is close to the experimental activation energy, $2.7 \pm 0.8$, $2.3 \pm 1.0$, and $3.2 \pm 0.2$ kcal/mol reported by Hayman et al.,[7] Clyne et al.,[3(b)] and Nickolaisen et al.,[13] respectively. IRC analysis[23] results

show that the forward side of TS3 connects to a loose complex, LM6, which is 1.0 kcal/mol lower than the $Cl_2 + {}^1O_2$ products.

On the triplet surface, the most likely process is that ClO and ClO form ${}^3cis$-ClOOCl (see Figs. 1 and 4) followed by dissociation to produce $Cl_2 + {}^3O_2$. However, the calculated result indicates that the formation of ${}^3cis$-ClOOCl occurs with a very high barrier, 28.6 kcal/mol. Formation of ${}^3trans$-ClOOCl (LM8) also has a similar high barrier, 28.0 kcal/mol, as shown in Fig. 4. Evidently, formation of triplet ClOOCl is energetically unfavorable. Similarly, trans- and cis-ClOClO (LM9, LM10) also have large entrance barriers, 28.1 and 33.4 kcal/mol, corresponding to TS6 and TS7, respectively. It should be mentioned that the high barriers for the entrance step on triplet potential energy surfaces were also found in the HO+ClO (Ref. 18) and HO+OClO (Ref. 16) reactions. For the HO+ClO→${}^3$HOOCl and HO+OClO→${}^3$HOOClO reactions, their barriers were found to be 17.2 (Ref. 18) and 35.0 (Ref. 16) kcal/mol, respectively. The transition state between ${}^3cis$-ClOOCl and $Cl_2 + {}^3O_2$ was not located at the B3LYP/6-311+G(3df) level of theory;

TABLE I. Vibrational frequencies and rotational constants for the reactants, the key intermediates, and transition states of the ClO+ClO reaction computed at the B3LYP/6-311+G(3df) level of theory.

| Species | B (GHZ) | Frequencies |
|---|---|---|
| ClO | 0.0, 18.5, 18.5 | 861.4 |
| ClOOCl[a] | 13.5, 2.3, 2.1 | 127 ($127 \pm 20$), 326, 443 (418), 551 (543), 638 (647, _648_), 844 (754, _752_) |
| ClOClO[a] | 14.9, 2.4, 2.2 | 116, 258, 354 (338.4), 441 (440.4), 622 (695.9), 1015 (994.5) |
| ClClO₂[b] | 9.4, 3.5, 2.7 | 243 (251.4), 264 (271.4), 441 (440.5), 524 (522.7), 1061 (1041.5), 1229 (1218) |
| OClClO | 14.4, 2.2, 2.1 | 87, 159, 209, 248, 934, 974 |
| OOClCl | 6.4, 2.8, 2.0 | 163, 226, 324, 501, 538, 1427 |
| TS1 | 19.6, 1.7, 1.6 | 159$i$, 125, 241, 444, 780, 926 |
| TS2 | 10.6, 2.5, 2.2 | 475$i$, 130, 226, 479, 981, 1211 |
| TS3 | 5.8, 3.2, 2.1 | 280$i$, 163, 249, 325, 557, 1386 |

[a]Italic and regular fonts of the frequencies in the parentheses are from the experimental results of Refs. 43 and 44, respectively.
[b]The frequencies in the parentheses are from the experimental results of Ref. 41.

TABLE II. Comparison of the predicted heats of formation of different species (at 0 K, in kcal/mol) in this work with available data.

| Species | Predicted | Expt. |
|---|---|---|
| ClOOCl | 29.4,[a] 29.4 (Ref. 33), 30.6 (Ref. 45), 32.6±3.2 (Ref. 30), 34.2 (Ref. 37) | 29.7 (Ref. 13), 32.1 (Ref. 9) |
| ClClO$_2$ | 29.8,[a] 33.8 (Ref. 30), 35.1 (Ref. 37), 37.1 (Ref. 33), 37.5 (Ref. 45) | |
| ClOClO | 36.4,[a] 42.4 (Ref. 45), 44.3 (Ref. 37) | |
| OClO | 23.2,[a] 24.7 (Ref. 19), 25.3 (Ref. 18), 28.2 (Ref. 45) | 23.7±1.9 (Ref. 46) |
| ClOO | 23.1,[a] 23.5 (Ref. 18), 30.2 (Ref. 45) | 23.8±0.7 (Ref. 46) |

[a]This work.

thus, the formation of $^3O_2$ from $^3cis$-ClOOCl may be a barrierless process.

### 3. Formation of ClOO+Cl and OClO+Cl

Besides the molecular elimination reaction producing $Cl_2 + {}^1O_2$, ClOOCl can also dissociate barrierlessly to give Cl+ClOO, as shown in Fig. 3. Similarly, triplet $cis$- and $trans$-ClOOCl (see Figs. 1 and 4) can dissociate to Cl +ClOO also but, as mentioned before, their high entrance barriers, 28.6 and 28.0 kcal/mol, corresponding to TS4 and TS5 (see Fig. 4), respectively, prevent the formation of Cl +ClOO via these triplet states.

The analogous reactions producing Cl+OClO, as shown in Figs. 3 and 4, can occur by the decomposition of ClOClO, ClClO$_2$, $^3cis$- and $^3trans$-ClOClO (LM9 and LM10). However, again, because of the high barriers at TS2, TS6, and TS7 (see Figs. 3 and 4), only the singlet ClOClO dissociation path will be discussed in the later rate constant calculation.

The endothermicities for the formation of Cl+ClOO and Cl+OClO are predicted to be 3.4 and 3.5 kcal/mol, respectively; these values can be compared with the activation energies 4.9±0.7 and 2.7±0.3 kcal/mol determined by Nickolaisen et al.[13] The heats of formation for the three lowlying Cl$_2$O$_2$ and ClO$_2$ isomers are discussed below.
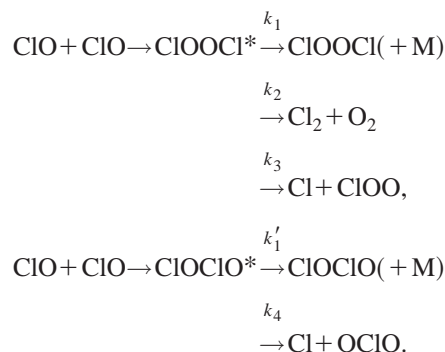
### 4. Heats of formation of ClOOCl, ClClO$_2$, ClOClO, ClOO, and OClO

In order to establish the reliability of the rate constant calculations, besides the comparison of the structural parameters, frequencies, and transition state barriers with available theoretical or experimental data given in the previous sections, here we also compare the heats of formation for some species with available values. The heats of formation at 0 K for ClO and Cl are known to be 24.15±0.024 and 28.59 ±0.0014, respectively.[46] Other heats of formation are calculated based on these values using the computed $\Delta_r H_0^o$. Table II presents the values and other calculated or experimental data for comparison. It can be seen that for ClOOCl, our result (29.4 kcal/mol) is close to those predicted by Stanton et al.[33] with the infinite-order coupled-cluster (CC) approximation and Li et al.[45] with the G2 method. All are in reasonable agreement with the experimental values, 29.7 (Ref. 13) and 32.1 (Ref. 9) kcal/mol. The highest value, 34.2 kcal/mol obtained by Lee et al.,[37] was based on the calculated enthalpy change for the isodesmic reaction, ClOOCl+H$_2$O =HOOH+Cl$_2$O, using the heat of formation of Cl$_2$O, 21.4

±1.6 kcal/mol. As stated in their *Note Added in Proof*,[37] if the recent value of $\Delta_f H_0^o$ (Cl$_2$O) = 19.8±0.5 kcal/mol[46] was used, the same isodesmic reaction led to 32.6±1.0 kcal/mol for the heat of formation for ClOOCl, which is consistent with 32.6±3.2 kcal/mol[30] predicted at the MP2/6-31+ +G(3$d$,2$p$) level based on the same isodesmic reaction. This lower value essentially overlaps with our value within the combined uncertainty in theory and experiment. Because of the high sensitivity of the predicted ClO+ClO association rates to the $D_0$ (ClO–OCl) value, we will compare the predicted rate constant as a function of $D_0$ in the next section. For ClClO$_2$ and ClOClO, there are large uncertainties; the maximum deviation among the results predicted by different methods reaches as much as 8 kcal/mol. For OClO and ClOO, our results 23.2 and 23.1 kcal/mol, are in good agreement with experimental values, 23.7±1.9 (Ref. 46) and 23.8±0.7 (Ref. 46), respectively; they are consistent with our previously predicted values based on the reactions $^3O$ +OClO→ClO+$^3O_2$[19] and HO+ClO→H+OClO,[18] 24.7 and 25.3 kcal/mol, respectively. It should be mentioned that the G2 method[45] overestimated the heats of formation of OClO and ClOO by 4.5 and 6.4 kcal/mol, respectively, compared with experimental values. The deviation may arise from the unreliable structures optimized at the MP2/6-31G($d$) level employed in the standard G2 method.

### B. Rate constant calculations

Variational TST and RRKM calculations have been carried out for the following reaction channels:

$$ClO + ClO \xrightarrow{k_1} ClOOCl^* \rightarrow ClOOCl(+M)$$

$$\xrightarrow{k_2} Cl_2 + O_2$$

$$\xrightarrow{k_3} Cl + ClOO,$$

$$ClO + ClO \xrightarrow{k_1'} ClOClO^* \rightarrow ClOClO(+M)$$
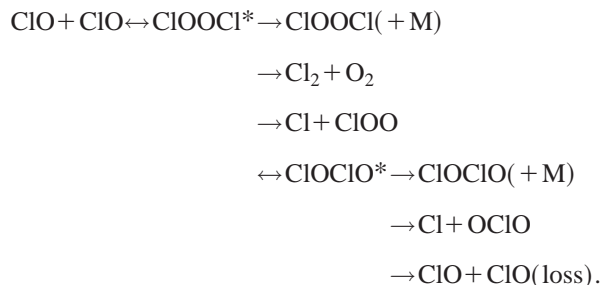
$$\xrightarrow{k_4} Cl + OClO.$$

The energies used in the calculation are plotted in Fig. 3 and the vibrational frequencies and rotational constants are listed in Table I. The LJ parameters required for the RRKM calculations for the quenching of ClOOCl*, $\varepsilon = 533$ K and $\sigma = 4.1$ Å, were derived from deconvoluting the LJ potential
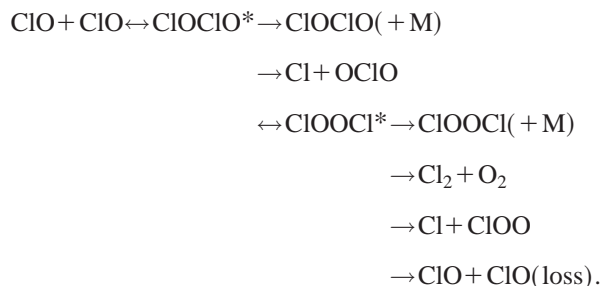
of the He–ClOOCl system obtained by our *ab initio* calculation at the B3LYP/6-311+G(3*df*) level. The $\varepsilon$ and $\sigma$ parameters for the He–ClOOCl collision pair were determined to be 73 K and 3.3 Å by fitting the LJ function,[47] $V = 4\varepsilon[(\rho/r)^{12} - (\sigma/r)^6]$. The LJ parameters for He, $\varepsilon = 10$ K and $\sigma = 2.55$ Å, were taken from the literature.[48]

The rate constants for the dominant association reactions ($k_1$ and $k_{1'}$) were calculated with the VARIFLEX code,[26] whereas those for the disproportionation reactions, $k_2$, $k_3$, and $k_4$, were computed with the CHEMRATE code[29] coupling all intermediates involved in the forward and reverse reactions as shown below:

*Scheme 1*:

$$ClO + ClO \leftrightarrow ClOOCl^* \rightarrow ClOOCl(+M)$$

$$\rightarrow Cl_2 + O_2$$

$$\rightarrow Cl + ClOO$$

$$\leftrightarrow ClOClO^* \rightarrow ClOClO(+M)$$

$$\rightarrow Cl + OClO$$

$$\rightarrow ClO + ClO(loss).$$

*Scheme 2*:

$$ClO + ClO \leftrightarrow ClOClO^* \rightarrow ClOClO(+M)$$

$$\rightarrow Cl + OClO$$

$$\leftrightarrow ClOOCl^* \rightarrow ClOOCl(+M)$$

$$\rightarrow Cl_2 + O_2$$

$$\rightarrow Cl + ClOO$$

$$\rightarrow ClO + ClO(loss).$$

In the CHEMRATE calculation, the transition state parameters for the barrierless association and decomposition processes were evaluated canonically for each temperature and critical separation, $r^{\#}(T)$, based on the maximum Gibbs free-energy criterion as described previously for radical–radical reactions.[49,50]

### 1. Pressure and third-body effects on formation of ClOOCl and ClOClO

The association of ClO radicals was found to be strongly pressure dependent.[11,13,15] The formation of both ClOOCl and ClOClO occurs barrierlessly; therefore, variational treatment was employed to obtain the dissociation potential energy function by varying the respective breaking O–O and Cl–O bonds from 1.361 to 4.161 Å and 1.723 to 3.723 Å at an interval of 0.1 Å; other geometry parameters were fully optimized at the B3LYP/6-311+G(3*df*) level. The computed potential energies could be fitted to the Morse function with the parameters $\beta = 1.498$ and 1.361 Å$^{-1}$ for the dissociation of ClO–OCl and ClO–ClO, respectively. Figures 5–7 show the predicted and experimental rate coefficients at different temperatures as a function of He, O$_2$, and N$_2$ pressure. In these figures, the solid, dash-dotted, dotted, and dashed curves correspond to the predicted values of the total rate constant $k_t$, $k_1$, $k_{1'}$, and ($k_2 + k_3 + k_4$), respectively. From these figures one can see most notably that $k_{1'}$ is not negli-
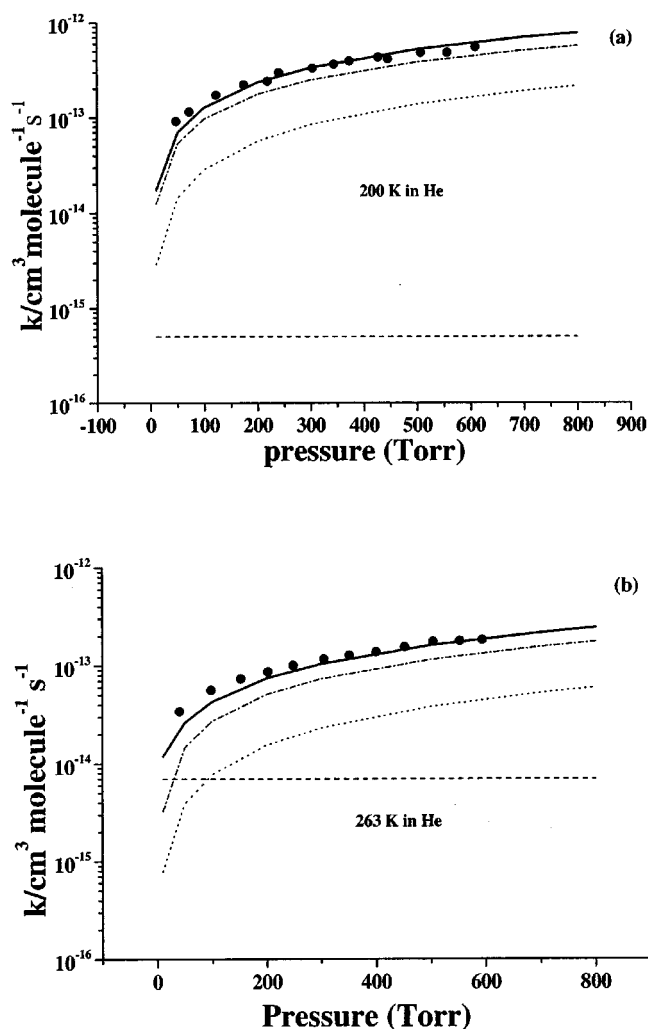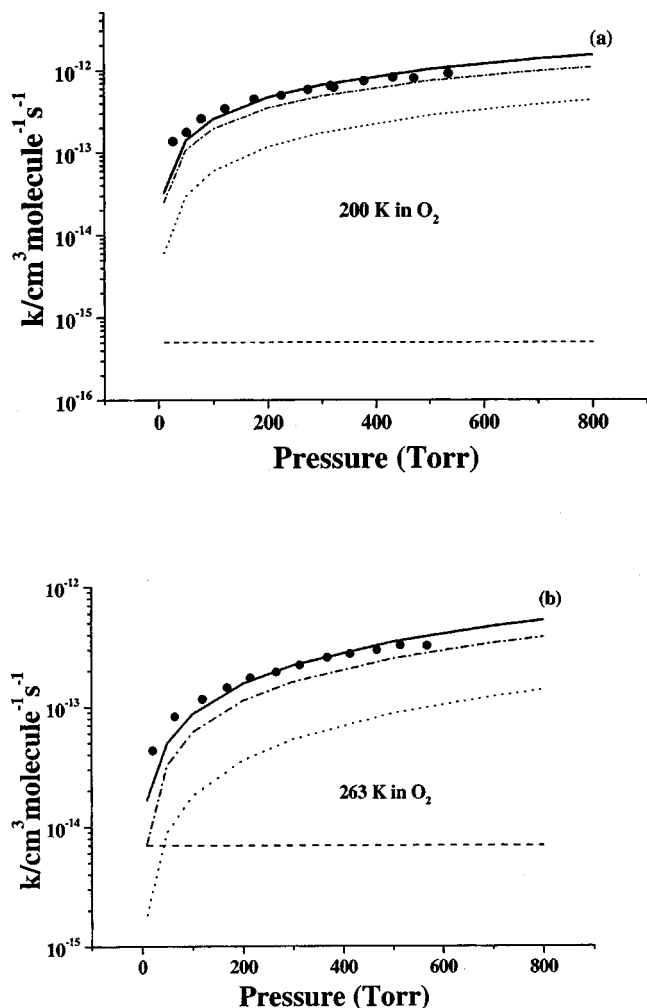


FIG. 5. Comparison of the predicted rate constants with the experimental values at 200 K (a) and 263 K (b) in He. Dashed, dotted, dash-dotted, and solid lines represent the predicted ($k_2 + k_3 + k_4$), $k_1'$, $k_1$, and $k_t$, respectively. ●, Ref. 11.

gible, for instance, accounting for about 18%–29% of the total rate from 10–800 Torr in N$_2$ at 200 K and that ($k_2 + k_3 + k_4$) is pressure independent and the association reactions forming ClOOCl and ClOClO are pressure dependent for all of the third bodies at all temperatures, with the former being dominant. The predicted total rate constants ($k_t$) are in excellent agreement with experimental data.[11,13,15] At higher temperatures (e.g., 263 K) and low pressures (<10 Torr), decomposition channels ($k_2 + k_3 + k_4$) become competitive, especially in He.

The third-body efficiencies of the buffer gases in this system are similar to those in the HO–CO system.[51] The predicted order of third-body efficiencies is SF$_6$>N$_2$≈O$_2$ >He with the values relative to N$_2$: 1.51 : 1.00 : 0.86 : 0.40 under the 263 K and 50–800 Torr conditions. The $\langle \Delta E_{\text{down}} \rangle$ used for fitting the experimental results in different third body is displayed in Table III, together with the modeled $k_0$ and $k_\infty$ in comparison with experimental results at 300 K for M=He, Ar, N$_2$, O$_2$, CF$_4$, and SF$_6$. It can be seen that the predicted $k^0$, the sum of $k_1^0$ and $k_{1'}^0$, is in good agreement with those experimental values[10,11,13] for different third bod-

FIG. 6. Comparison of the predicted rate constants with the experimental values at 200 K (a) and 263 K (b) in $O_2$. Dashed, dotted, dash-dotted, and solid lines represent the predicted $(k_2+k_3+k_4)$, $k_1'$, $k_1$, and $k_t$, respectively. ●, Ref. 11.



FIG. 7. The variation of the predicted rate constants with $D_0$ (ClO–OCl) at 200 K (a) and 263 K (b) in $N_2$. Solid, dashed, dotted lines 1, 2, 3 represent the predicted $k_t$ using $D_0=18.9$, 16.3, and 14.1 kcal/mol for ClOOCl association process, respectively; lines 4 and 5 represent $k_1'$ and $(k_2+k_3+k_4)$; symbols are the experimental values. ●, Ref. 11; △, Ref. 13 at 208 K; △, Ref. 13 at 195 K.

ies; $k^\infty(k_1^\infty+k_{1'}^\infty)$ is, however, about 1 order of magnitude larger than the experimentally extrapolated values,[11,13] suggesting that the extrapolation is likely insufficient due to the lack of data in the higher pressure regime. A similar observation was made in our study of the O+OClO reaction.[19]

It is clear that in order to well present the experimental results, the ClOClO formation channel should be taken into account (see Figs. 5–7) and that single Troe fits to these fall-off data cannot be quantitatively employed for interpolation or extrapolation of $P$-dependent data. In addition, the high-pressure limits obtained from these data in the rather narrow $P$ range are not reliable as mentioned above.

Although the formation of bimolecular products (Cl +OClO/ClOO and $Cl_2+O_2$) from the ClO+ClO reaction is insensitive to the value of the well depth, $D_0$(ClO–OCl), the rate constant for the formation of ClOOCl is, however, very sensitive on account of the relatively shallow well. In view of the spread of the $D_0$ values, from 18.9 to 14.1 kcal/mol as alluded to above, we have compared the predicted bimolecular rate constants for the ClO+ClO reaction with three different dissociation energies at 200 and 263 K in $N_2$ as shown in Figs. 7(a) and 7(b). In these figures, lines 1, 2, and 3 rep-
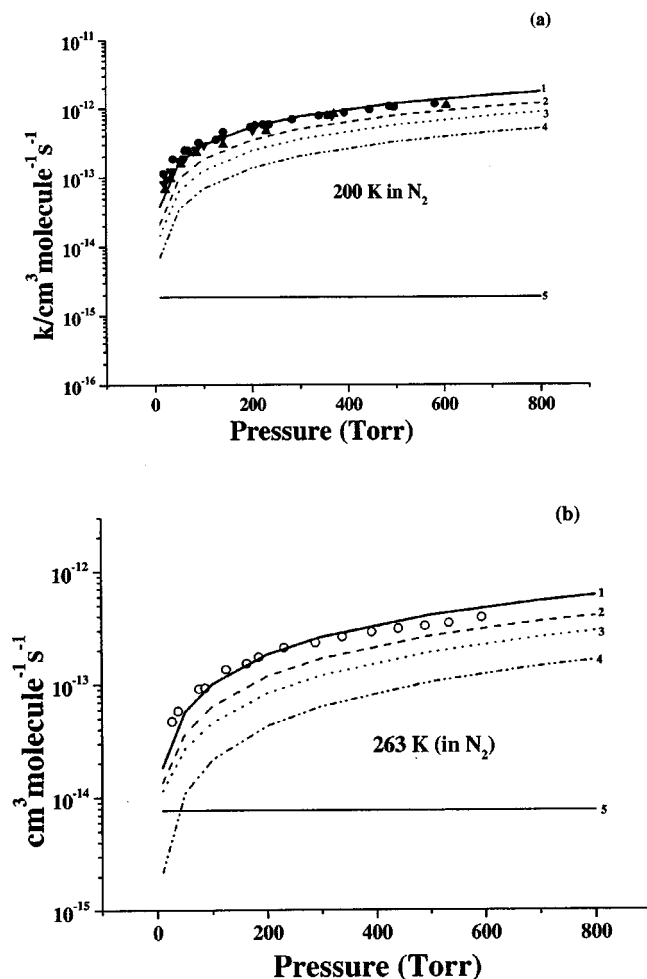
resent the $k_t$ predicted by $D_0$(ClO–OCl)=18.9, 16.3, and 14.1 kcal/mol; lines 4 and 5 represent $k_1'$ and $(k_2+k_3+k_4)$, which are included in the total rate constant. Evidently, the lower values of $D_0$ (14.1 and 16.3 kcal/mol) underpredict the bimolecular rates due to the faster back-dissociation of the excited ClOOCl*. For example, with $D_0=16.3$ and 14.1 kcal/mol at 263 K, the predicted total rate constants decrease by as much as 34% and 52% in the pressure range of 50–800 Torr, respectively, comparing with the value calculated with $D_0=18.9$ kcal/mol, which agrees closely with experimental data as illustrated above. An additional comparison will be made below using five independent sets of experimental data over a wide range of temperatures.

For practical applications, we have analyzed our theoretical fall-off curves in terms of the following empirical equations to obtain broadening parameters ($F_c$):[52,53]

$$k=a[b/(1+b)]F,$$

$$\log F=\log F_c/[1+(\log b)^2],$$

TABLE III. Comparison of the predicted and experimental $k^\infty$ and $k^0$ in different third bodies for ClO+ClO →Cl$_2$O$_2$+M at 300 K.

| M | P/Torr | $k^a$ | $\langle \Delta E_{down} \rangle$ cm$^{-1}$ |
|---|---|---|---|
| He | 0 | 0.74,[b] 0.99±(0.05) (Ref. 13), 0.46±0.04 (Ref. 11) | 120 |
| Ar | 0 | 1.34,[b] 1.71±0.06 (Ref. 13) | 400 |
| N$_2$ | ∞ | 87,[b] (6±2) (Ref. 13), 8.0 (Ref. 11) | |
| N$_2$ | 0 | 1.85,[b] 1.96±0.24 (Ref. 13), 1.8±0.5 (Ref. 10), 1.34 ±0.09 (Ref. 11) | 400 |
| O$_2$ | 0 | 1.54,[b] 1.24±0.09 (Ref. 13), 1.10±0.08 (Ref. 11), 1.7 ±0.5 (Ref. 10) | 350 |
| CF$_4$ | 0 | 2.1,[b] 2.6±0.17 (Ref. 13) | 500 |
| SF$_6$ | 0 | 3.37,[b] 3.15±0.14 (Ref. 13), 2.22±0.14 (Ref. 11) | 1000 |

[a]$k$, the sum of $k_1$ and $k_{1'}$; is given in units of $10^{-32}$ cm$^6$ molecule$^{-2}$ s$^{-1}$ for $k^0$ and $10^{-12}$ cm$^3$ molecule$^{-1}$ s$^{-1}$ for $k^\infty$.
[b]This work.

using the predicted high- and low-pressure limits for N$_2$ as the third body. For the ClOOCl association path, we obtained $F_c$=0.24, 0.22, 0.22, and 0.27 at 200, 263, 298, and 400 K, respectively. In the fitting, $a=k^\infty$=3.40, 3.07, 2.90, and 2.51 in units of $10^{-11}$ cm$^3$ molecule$^{-1}$ s$^{-1}$, and $b=k^0[\text{M}]/k^\infty$ with $k^0$=6.19, 2.35, 1.47, and 0.464 in units of $10^{-32}$ cm$^6$ molecule$^{-2}$ s$^{-1}$, respectively. For the ClOClO association path, $F_c$=0.72, 0.74, 0.75, and 0.83 at 200, 263, 298, and 400 K with $a=k^\infty_{-1}$=6.97, 6.19, 5.80, and 4.90 in units of $10^{-11}$ cm$^3$ molecule$^{-1}$ s$^{-1}$ and $k^0_{-1}$=14.5, 5.94, 3.83, and 1.23 in units of $10^{-33}$ cm$^6$ molecule$^{-2}$ s$^{-1}$, respectively.

### 2. Temperature effect

*a. Association/decomposition processes.* Under the condition of interest to the stratosphere O$_3$ chemistry, the ClO +ClO reaction is dominated by the association and decomposition processes. In Fig. 8, the predicted and experimental rate constants for the association processes in N$_2$ as a func-
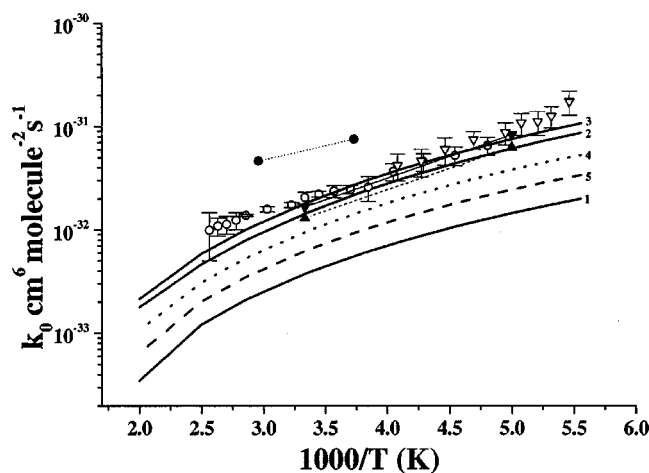


FIG. 8. Comparison of the predicted third-order rate constants with the experimental values in N$_2$. Lines 1, 2, and 3 represent the predicted formation rate constants of ClOClO, ClOOCl, and their sum, i.e., $k'_1$, $k_1$, and $k_1+k'_1$; dotted and dashed lines 4, and 5 represent the predicted $k_t$ using $D_0$=16.3 and 14.1 kcal/mol for ClOOCl association process, respectively; symbols are the experimental values ○, Ref. (13); ---●---, Ref. 7; ---▲---, Ref. 11; --▼--, Ref. 55; ▽, Ref. 15.

tion of temperature are plotted and compared. It can be seen that the total rate constants for the formation of ClOOCl and ClOClO computed with our predicted dissociation energies for both molecules are in reasonable agreement with experimental results given by Trolier *et al.*,[11] Nickolaisen *et al.*,[13] Bloss *et al.*,[15] and Atkinson *et al.*;[54] they are, however, about one order of magnitude lower than that reported by Hayman *et al.*[7] in a similar temperature range. The predicted second- and third-order rate constants for formation of ClOOCl and ClOClO can be expressed, respectively, by

$$k_1^\infty = 1.6 \times 10^{-9} T^{-0.67} \exp(-64/T) \text{cm}^3 \text{ molecule}^{-1} \text{ s}^{-1},$$

$$k_{1'}^\infty = 6.4 \times 10^{-9} T^{-0.78} \exp(-76/T) \text{cm}^3 \text{ molecule}^{-1} \text{ s}^{-1},$$

$$k_1^0 = 8.31 \times 10^{-20} T^{-4.96} \exp(-336/T) \text{cm}^6 \text{ molecule}^{-2} \text{ s}^{-1},$$

$$k_{1'}^0 = 1.72 \times 10^{-14} T^{-6.99} \exp(-926/T) \text{cm}^6 \text{ molecule}^{-2} \text{ s}^{-1},$$

for the temperature range 180–500 K. Similarly, the unimolecular decomposition rate constants for the dissociation of ClOOCl and ClOClO can be given by the following expressions for the high- and low-pressure limits:

$$k_{-1}^\infty = 6.3 \times 10^{19} T^{-1.32} \exp(-9999/T) \text{s}^{-1},$$

$$k_{1'}^\infty = 5.99 \times 10^{20} T^{-1.63} \exp(-6474/T) \text{s}^{-1},$$

$$k_1^0 = 4.64 \times 10^8 T^{-5.2} \exp(-10\,159/T) \text{cm}^3 \text{ molecule}^{-1} \text{ s}^{-1},$$

$$k_{-1'}^0 = 6.81 \times 10^6 T^{-4.9} \exp(-6488/T) \text{cm}^3 \text{ molecule}^{-1} \text{ s}^{-1}.$$

The optical isomers of ClOOCl have been considered in the prediction of ClOOCl dissociation constant.

In Fig. 8, we have also compared the predicted total third-order rate constants (dotted and dashed lines 4 and 5) with $D_0$(ClO−OCl)=16.3 and 14.1 kcal/mol. These lower values of dissociation energy again underpredict the third-order rate constant noticeably; at 200 K, for example, the predicted values are a factor of 2 and 3, respectively, below experimental data, which agree quantitatively with the result calculated with the 18.9 kcal/mol dissociation energy evaluated by the G2M method.

*b. Equilibrium constants.* $K_{1p}$ and $K_{1'p}$. The predicted equilibrium constants for reactions (1) and (1')
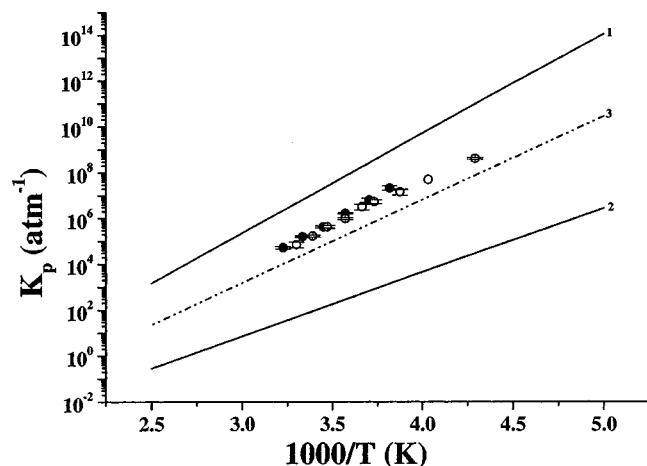
FIG. 9. Comparison of the predicted temperature dependence for equilibrium constants $K_{1p}$ and $K_{1'p}$ with experimental values. -●-, Ref. 13; -○-, Ref. 9. The meanings of lines 1–3 can be found in the related part in the text.



FIG. 10. Comparison of the predicted bimolecular reaction rate constant for $ClO+ClO \rightarrow Cl_2+O_2$ with the experimental values. Solid line is the predicted total value coupling Schemes 1 and 2; dotted line is the contribution from Scheme 2. -●-, Ref. 55; -▲-, Ref. 13; ⊕, Ref. 12; △, Ref. 6; □, Ref. 5; ×, Ref. 56; ▽, Ref. 57; ▼; Ref. 58.

$$ClO+ClO=ClOOCl, \qquad (1)$$

$$ClO+ClO=ClOClO, \qquad (1')$$

are shown in Fig. 9 by solid lines 1 and 2, respectively, for comparison with experimental values assuming the presence of only reaction (1). The predicted $K_{1p}$ is apparently larger than experimental values[9,13] by almost 2 orders of magnitude, whereas $K_{1'p}$ is lower by 3–5 orders of magnitude in the experimental temperature range based on the predicted enthalpy changes, $-18.9$ and $-11.9$ kcal/mol, respectively. The total $K_p$ (dash-dot-dotted line 3) predicted by Slanina and Filip[36] using $\Delta_1 H_0^o \sim -16.1$ kcal/mol including the three stable isomers (ClOOCl, ClOClO, and ClClO$_2$) is also compared in Fig. 9; their result is about one and half orders of magnitude lower than the experimental values. As our predicted pressure dependence and the third-body effect on the association rate constants at different temperatures using the predicted enthalpy changes, $\Delta_1 H_0^o = -18.9$ and $\Delta_{1'} H_0^0 = -11.9$ kcal/mol, are quite reasonable, the deviation results most likely from the contributions of reaction (1') (which was not included in all previous kinetic data analyses) and radical reactions involving ClOOCl. Slanina and Filip[36] assumed that ClClO$_2$ could contribute to the total observed $K_p$, but from the calculated PES we see that ClClO$_2$ is not easily accessible from ClO+ClO due to the high isomerization barrier at TS2 (see Fig. 3); its contribution to the total $K_p$ may be neglected.

*c. Cl$_2$+O$_2$ formation.* The reported rate constant for the formation of Cl$_2$+O$_2$ exhibits an order of magnitude scatter at 298 K.[5,6,12,13,54–58] As described in the *ab initio* calculation part, ClOOCl can dissociate to Cl$_2$+O$_2$ via a four-center transition state TS3 with a barrier of 3.6 kcal/mol above the reactants. With this barrier height, the result of our CHEMRATE calculation based on Schemes 1 and 2 given above, as shown in Fig. 10, is in reasonable agreement with the values reported by DeMore *et al.*[55] and Simon *et al.*[12] at low temperature, but the model slightly overestimated at high temperatures compared with the most recent experimen-
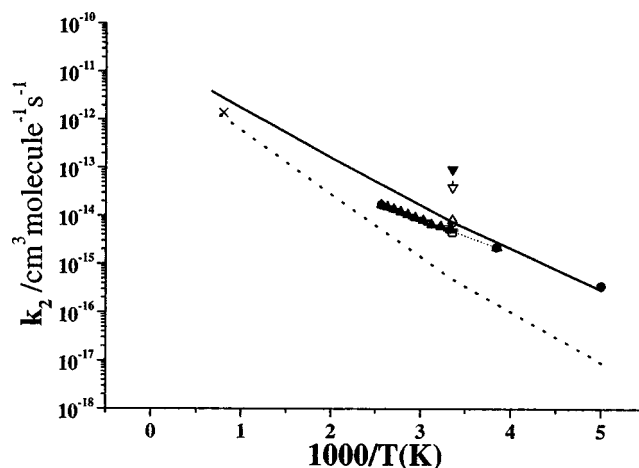
tal values of Nickolaisen *et al.*[13] However, at 1250 K, our predicted value is close to the one given by Park.[56]

The predicted $k_2$ can be expressed by $k_2 = 1.09 \times 10^{-13} T^{0.66} \exp(-1892/T)$ cm$^3$ molecule$^{-1}$ s$^{-1}$. For comparison, the contribution from Scheme 2 is also shown as a dotted line in Fig. 10. The result indicates that below 298 K, the indirect contribution from Scheme 2 to $k_2$ via ClOClO* is less than 7%; however, at higher temperatures, the contribution increases and reaches around 40% at 1500 K.

*d. Cl+ClOO formation.* ClOOCl can also dissociate barrierlessly to produce Cl+ClOO without a well-defined transition state. The variational potential energies were obtained by varying the breaking O–Cl bond from 1.748 to 3.548 Å at an interval of 0.1 Å. The computed potential
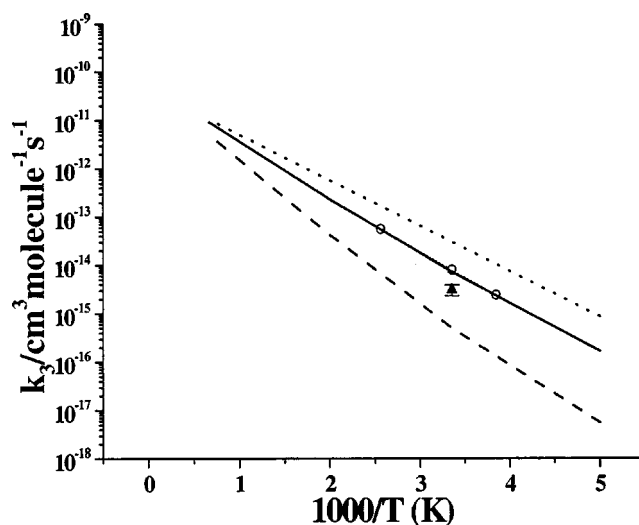


FIG. 11. Comparison of the predicted bimolecular reaction rate constant for $ClO+ClO \rightarrow Cl+ClOO$ with the experimental values. Dotted and solid lines are calculated by using predicted 23.1 and experimental 23.8 kcal/mol for the heat of formation for ClOO, respectively. Dashed line is the contribution from Scheme 2 using the experimental heat of formation for ClOO. -○-, Ref. 13; -▲-, Ref. 5.
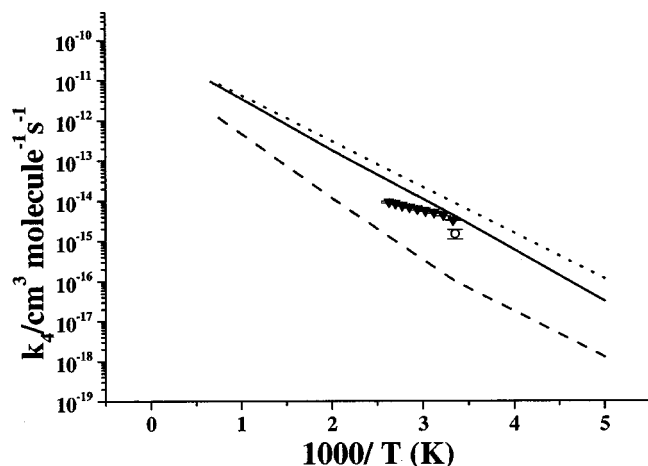
FIG. 12. Comparison of the predicted bimolecular reaction rate constant for $ClO+ClO\rightarrow Cl+OClO$ with the experimental values. Dotted and solid lines are calculated by using predicted 23.2 and experimental 23.7 kcal/mol for the heat of formation for ClOO, respectively. Dashed line is the contribution from Scheme 1 using the experimental heat of formation for ClOO. -●-, Ref. 13; -○-, Ref. 5.

energies could be fitted to the Morse function with the parameter, $\beta=3.343$ Å$^{-1}$. The predicted and experimental heats of formation for ClOO, 23.1 and 23.8 kcal/mol, were both used in the rate constant calculation. The results are given by dotted and solid curves, respectively, in Fig. 11. The latter, obtained with the experimental heat of formation for ClOO, is shown to give a much better agreement with experimental data. The obvious deviation between the two theoretical curves stemming from a rather small difference in the endothermicity employed, 0.7 kcal/mol, clearly illustrates the sensitivity of the computed rate constants to the predicted energetics. The result corresponding to the solid curve can be expressed by $k_3=1.36\times10^{-13}\,T^{0.77}\exp(-2168/T)$ cm$^3$ molecule$^{-1}$ s$^{-1}$, covering the temperature range 200–1500 K. The small contribution from Scheme 2 to $k_3$, similar to that for $Cl_2+O_2$ formation, is shown as a dashed line in Fig. 11.

*e. Cl+OClO formation.* In principle, Cl+OClO can be formed by the dissociation of ClOClO and ClClO$_2$; however, due to the higher isomerization barrier from ClOClO to ClClO$_2$ (see Fig. 3), formation of Cl+OClO from ClClO$_2$ can be neglected. For the decomposition of ClOClO, the variational potential energies were obtained by varying the breaking O–Cl bond from 1.720 to 5.12 Å at an interval of 0.1 Å, and $\beta=1.732$ Å$^{-1}$ is determined by fitting the calculated potential to the Morse function. Figure 12 compares the predicted data with experimental values. The dotted and solid lines represent the results by using the predicted and experimental heats of formation for OClO, 23.2 and 23.7 kcal/mol, respectively. The latter result indicates that the predicted values given by $k_4=6.26\times10^{-11}\,T^{0.005}\times\exp(-2896/T)$ cm$^3$ molecule$^{-1}$ s$^{-1}$ covering the temperature range of 200 and 1500 K are in close agreement with the reported data by Cox and Derwent[5] and Nickolaisen et al.[13] at lower temperatures, but deviate noticeably from experimental values at higher temperatures. The deviation may arise in part from the large uncertainty in the heat of forma-
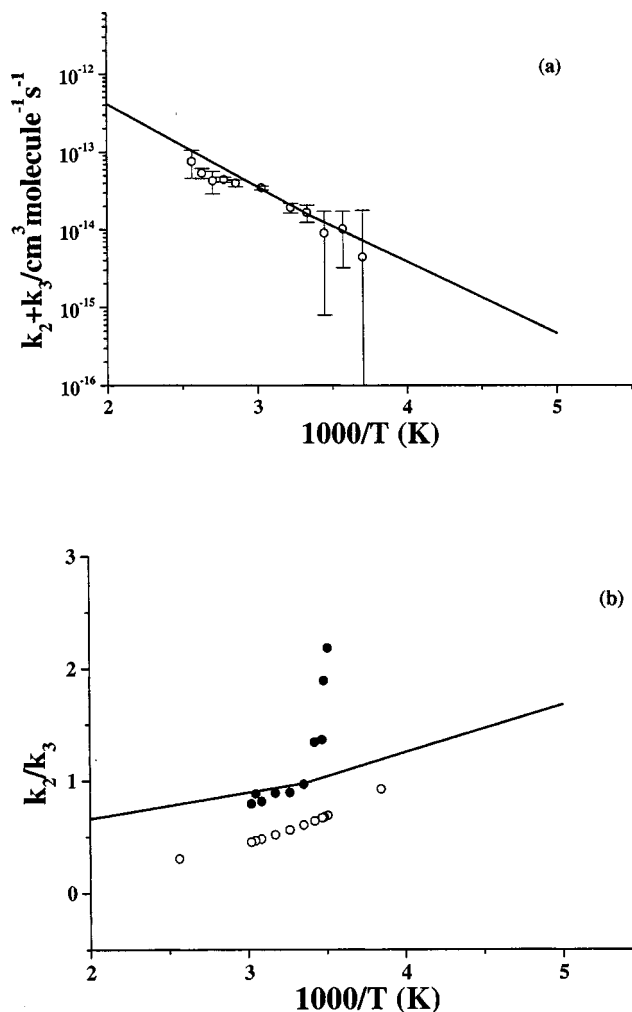




FIG. 13. Comparison of the predicted (a) $k_2+k_3$ and (b) $k_2/k_3$ with experimental values. Solid line is the predicted result. ○, Ref. 13; ●, Ref. 14.

tion of OClO, $23.7\pm1.9$ kcal/mol[46] (see Table II). In Fig. 12, we also present the indirect contribution from Scheme 1 to $k_4$, shown as a dashed line. The result suggests that the isomerization between ClOOCl* and ClOClO* has a minor effect on $k_4$, less than 5% below room temperature.

### 3. Comparison of $k_2+k_3$ and $k_2/k_3$ with experimental values

Experimentally, Nickolaisen et al.[13] and Horowitz et al.[14] reported the directly measured results for $k_2+k_3$ and $k_2/k_3$ in the temperature ranges of 270–390 K and 285–331 K, under the corresponding pressures of 1–36 and 503–576 Torr, respectively. Figures 13(a) and 13(b) compare the predicted and experimental data. It can be seen from Fig. 13(a) that the predicted values for $k_2+k_3$ agree closely with the result of Nickolaisen et al.[13] The predicted $k_2/k_3$ ratios lie between the values reported by Horowitz et al.[14] and those calculated with the individual $k_2$ and $k_3$ obtained by Nickolaisen et al.[13] The large scatter in the experimental results reflects the difficulty in determining the product branching ratios experimentally.
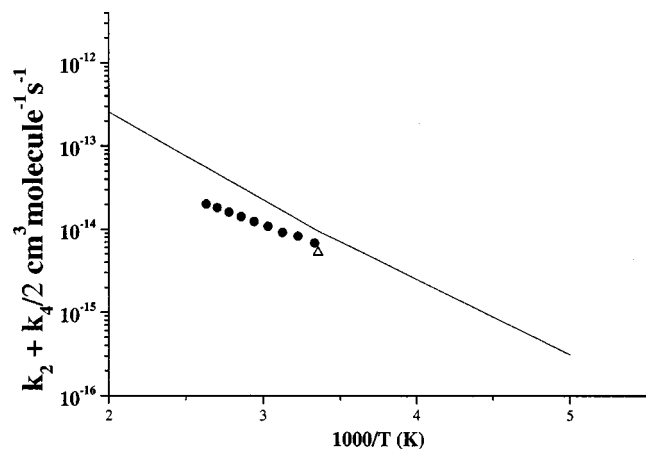
FIG. 14. Comparison of the predicted $k_2 + k_4/2$ with experimental values. Solid line is the predicted result. ●, Ref. 13. △, Ref. 5.

## 4. Comparison of $k_2 + k_4/2$ with experimental values

Figure 14 shows the comparison of the predicted $k_2 + k_4/2$ with experimental results of Nickolaisen et al.[13] As already shown in Figs. 10 and 12, at high temperatures theory overestimated both $k_2$ and $k_4$; this is also reflected in the comparison. The differences between the predicted and experimental values of $k_2$ and $k_4$ could be attributed to the difficulty in differentiating experimentally the reaction products, particularly $Cl_2 + O_2$ versus $Cl + ClOO$ (whose reaction quickly generates the former product pair). Take the result at 298 K as an example; the product branching ratios for $Cl_2 + O_2$, $Cl + ClOO$, and $Cl + OClO$ estimated by Cox and Derwent,[5] Simon et al.,[12] Nickolaisen et al.,[13] and Horowitz et al.,[14] vary noticeably: $(0.49 \pm 0.11, 0.34 \pm 0.09, 0.17 \pm 0.05)$; $(0.33 \pm 0.08, 0.33 \pm 0.07, 0.34 \pm 0.12)$; $(0.30, 0.49, 0.21)$; and $(0.39, 0.40, 0.20)$, respectively. The ratio predicted in this work $(0.39, 0.40, 0.21)$, is in reasonable agreement with those reported by Nickolaisen, Horowitz, and co-workers.

## IV. CONCLUDING REMARKS

The kinetics and mechanism for the self-reaction of ClO radicals have been investigated at the G2M/B3LYP/6-311 +G($3df$) level of theory in conjunction with statistical rate constant calculations. Experimentally determined rate constants for the bimolecular association process producing $Cl_2O_2$ could be quantitatively accounted for only with the inclusion of both ClOOCl and ClOClO dimer products. The latter accounts for about 23% of the dimer yield at 200 K and 22% at room temperature at 100 Torr $N_2$. The rate constants for the formation of $Cl_2 + O_2$ ($k_2$), $Cl + ClOO$ ($k_3$), and $Cl + OClO$ ($k_4$), could be reasonably accounted for theoretically, however, with noticeable overestimation in $k_2$ and $k_4$, compared with those reported recently by Sander and co-workers.[13] The origins of the deviations, aside from the potential predictive error of the theory in energetics ($\pm 1$ kcal/mol based on the heats of formation obtained computationally for OClO, ClOO, and ClOOCl), omissions of many important stable species in kinetic modeling of experimen-

tally measured data might also have contributed to errors in evaluating rate constants and product branching ratios. For example

$$Cl + OClO + M \rightarrow ClClO_2 + M,$$

$$ClO + OClO + M \rightarrow ClOClO_2 + M, \quad \text{etc.}$$
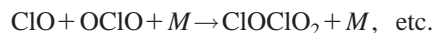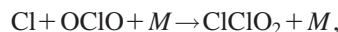
The formation of these and other stable intermediates (such as ClOClO) and their reactions with Cl, ClO, and OClO may significantly affect the predicted concentrations of these reactive species, which were monitored experimentally in most kinetic studies. To reliably examine the effects of these and other $ClO_x$ reactions, efforts are under way to calculate the rate constants for the association of Cl and ClO with OClO and the reactions of $Cl_2O_2$ and $Cl_2O_3$ isomers with these radicals.

Finally, it should be mentioned that although all existing kinetic data for the recombination and disproportionation reactions of ClO radicals could be quantitatively accounted for with our predicted energies within $\pm 1.0$ kcal/mol, the obvious discrepancy between the heat of formation of ClOOCl derived from the computed dimerization energy, $\Delta_f H_0^o$ (ClOOCl) = 29.4 kcal/mol, and the value estimated by a presumably more reliable isodesmic calculation based on the $Cl_2O + HOOH = ClOOCl + H_2O$ reaction, $32.6 \pm 1.0$ kcal/mol, deserves further investigation. The latter, larger heat of formation significantly underpredicts the independently determined, more reliable recombination kinetic data by several research groups.

[1] R. S. Stolarski and R. J. Cicerone, Can. J. Chem. **52**, 1610 (1974).
[2] F. S. Rowland and M. J. Molina, Rev. Geophys. Space Phys. **78**, 5341 (1975); F. S. Rowland, Annu. Rev. Phys. Chem. **42**, 731 (1991); H. S. Johnston, ibid. **43**, 1 (1992).
[3] (a) M. A. A. Clyne, D. J. McKenney, and R. T. Watson, J. Chem. Soc., Faraday Trans. 1 **71**, 322 (1975); (b) M. A. A. Clyne, D. J. McKenney, and R. T. Watson, ibid. **73**, 1169 (1977).
[4] N. Basco and J. Hunt, Int. J. Chem. Kinet. **11**, 649 (1979).
[5] R. A. Cox and R. G. Derwent, J. Chem. Soc., Faraday Trans. 1 **75**, 1635 (1979).
[6] J. P. Burrows and R. A. Cox, J. Chem. Soc., Faraday Trans. 1 **77**, 2465 (1981).
[7] G. D. Hayman, J. M. Davies, and R. A. Cox, Geophys. Res. Lett. **13**, 1347 (1986).
[8] L. T. Molina and L. J. Molina, J. Phys. Chem. **91**, 43743 (1987).
[9] R. A. Cox and G. D. HayMan, Nature (London) **332**, 796 (1988).
[10] S. P. Sander, R. Friedl, and Y. L. Young, Science **245**, 1095 (1989).
[11] M. Trolier, R. L. Mauldin III, and A. R. Ravishankara, J. Phys. Chem. **94**, 4896 (1990).
[12] F. G. Simon, W. Schneider, G. K. Moortgat, and J. P. Burrows, J. Photochem. Photobiol., A **94**, 4896 (1990).
[13] S. L. Nickolaisen, R. R. Friedl, and S. P. Sander, J. Phys. Chem. **98**, 155 (1994).
[14] A. Horowitz, J. N. Crowley, and G. K. Moortgat, J. Phys. Chem. **98**, 11924 (1994).
[15] W. J. Bloss, S. L. Nickolaisen, R. J. Salawitch, R. R. Friedl, and S. P. Sander, J. Phys. Chem. A **105**, 11226 (2001).
[16] Z. F. Xu, R. S. Zhu, and M. C. Lin, J. Phys. Chem. (submitted).

[17] R. S. Zhu and M. C. Lin, PhysChemComm **25**, 1 (2001).

[18] R. S. Zhu, Z. F. Xu, and M. C. Lin, J. Chem. Phys. **116**, 7452 (2002).

[19] R. S. Zhu and M. C. Lin, J. Phys. Chem. A **106**, 8386 (2002).

[20] A. D. Becke, J. Chem. Phys. **98**, 5648 (1993).

[21] A. D. Becke, J. Chem. Phys. **96**, 2155 (1992); **97**, 9173 (1992).

[22] C. Lee, W. Yang, and R. G. Parr, Phys. Rev. B **37**, 785 (1988).

[23] C. Gonzalez and H. B. Schlegel, J. Phys. Chem. **90**, 2154 (1989).

[24] A. M. Mebel, K. Morokuma, and M. C. Lin, J. Chem. Phys. **103**, 7414 (1995).

[25] M. J. Frisch, G. W. Trucks, H. B. Schlegel *et al.*, GAUSSIAN 98, Revision A.1, Gaussian, Inc., Pittsburgh, PA, 1998.

[26] S. J. Klippenstein, A. F. Wagner, R. C. Dunbar, D. M. Wardlaw, and S. H. Robertson, VARIFLEX: Version 1.00, 1999.

[27] R. G. Gilbert and S. C. Smith, *Theory of Unimolecular and Recombination Reactions* (Blackwell Scientific, Carlton, Australia, 1990).

[28] K. A. Holbrook, M. J. Pilling, and S. H. Robertson, *Unimolecular Reactions* (Wiley, New York, 1996).

[29] V. Mokrushin, V. Bedanov, W. Tsang, M. R. Zachariah, and V. D. Knyazev, CHEMRATE, Version 1.19, National Institute of Standards and Technology, Gaithersburg, MD 20899, 2002.

[30] M. P. McGrath, K. C. Clemitshaw, F. S. Rowland, and W. J. Hehre, Geophys. Res. Lett. **15**, 883 (1988).

[31] M. P. McGrath, K. C. Clemitshaw, F. S. Rowland, and W. J. Hehre, J. Phys. Chem. **94**, 6126 (1990).

[32] F. Jensen and J. Oddershede, J. Phys. Chem. **94**, 2235 (1990).

[33] J. F. Stanton, C. M. L. Rittby, R. J. Bartlett, and D. W. Toohey, J. Phys. Chem. **95**, 2107 (1991).

[34] A. P. Rendell and T. J. Lee, J. Chem. Phys. **94**, 6219 (1991).

[35] Z. Slanina and F. Uhlik, J. Phys. Chem. **95**, 5432 (1991).

[36] Z. Slanina and F. Uhlik, Chem. Phys. Lett. **182**, 51 (1991); Geophys. Res. Lett. **18**, 1703 (1991).

[37] T. J. Lee, C. M. Rohlfing, and J. E. Rice, J. Chem. Phys. **97**, 6593 (1992).

[38] D. Christen, H. G. Mack, and H. S. P. Müller, J. Mol. Struct. **509**, 137 (1999).

[39] M. Birk, R. R. Friedl, E. A. Cohen, H. M. Pickett, and S. P. Sander, J. Chem. Phys. **91**, 6588 (1989).

[40] H. S. P. Müller and E. A. Cohen, J. Phys. Chem. A **101**, 3049 (1997).

[41] H. S. P. Müllerand H. Willner, Inorg. Chem. **31**, 2527 (1992).

[42] F. Jensen and J. Oddershede, J. Phys. Chem. **94**, 2235 (1990).

[43] B. M. Cheng and Y. P. Lee, J. Chem. Phys. **90**, 5930 (1989).

[44] J. Jacobs, M. Kronberg, H. S. P. Müller, and H. Willner, J. Am. Chem. Soc. **116**, 1106 (1994).

[45] W. K. Li and C. Y. Ng, J. Phys. Chem. A **101**, 113 (1997).

[46] M. W. Chase, Jr., *NIST-JANAF Thermochemical Tables*, 4th ed. (AIP, Woodbury, NY, 1998).

[47] J. O. Hirschfelder, C. F. Curtiss, and R. B. Bird, *Molecular Theory of Gases and Liquids*, 2nd ed. (Wiley, New York, 1964).

[48] H. Hippler, J. Troe, and H. J. Wendelken, J. Chem. Phys. **78**, 6709 (1983).

[49] C.-C. Hsu, A. M. Mebel, and M. C. Lin, J. Chem. Phys. **105**, 2346 (1996).

[50] D. Chakraborty, C.-C. Hsu, and M. C. Lin, J. Chem. Phys. **109**, 8887 (1998).

[51] R. S. Zhu, E. G. W. Diau, M. C. Lin, and A. M. Mebel, J. Phys. Chem. A **105**, 11249 (2001).

[52] J. Troe, J. Phys. Chem. **83**, 114 (1979).

[53] J. Troe, Ber. Bunsenges. Phys. Chem. **87**, 161 (1983); R. G. Cilbert, K. Luther, and J. Troe, *ibid.* **87**, 169 (1983).

[54] R. Atkinson, D. L. Baulch, R. A. Cox, R. F. Hampson, Jr., J. A. Kerr, M. J. Rossi, and J. Troe, J. Phys. Chem. Ref. Data **26**, 521 (1997).

[55] W. B. DeMore, S. P. Sander, D. M. Golden, R. F. Hampson, M. J. Kurylo, C. J. Howard, A. R. Ravishankara, C. E. Kolb, and M. J. Molina, JPL Publication 97-4 (1997).

[56] C. Park, J. Phys. Chem. **80**, 565 (1976).

[57] F. H. C. Edgecombe, R. G. W. Norrish, F. R. S. Thrush, and B. A. Thrush, Proc. R. Soc. London, Ser. A **243**, 24 (1957).

[58] F. J. Lipscomb, R. G. W. Norrish, and G. Porter, Nature (London) **174**, 785 (1954).